Resonance Raman Spectroscopy of Blue Copper Proteins: Ligand and Coenzyme Effects in Copper(II)-Substituted Liver Alcohol Dehydrogenase

Wolfgang Maret,[1a] Andrew K. Shiemke,[1b] William D. Wheeler,[1b] Thomas M. Loehr,[1b] and Joann Sanders-Loehr*[1b]

Contribution from Fachbereich 15.2, Analytische und Biologische Chemie, Universität des Saarlandes, D-6600 Saarbrücken 11, FRG, and the Department of Chemical, Biological, and Environmental Sciences, Oregon Graduate Center, Beaverton, Oregon 97006-1999.
Received July 5, 1985

Abstract: Liver alcohol dehydrogenase with Cu(II) substituted for the native Zn(II) at the catalytic metal site exhibits a resonance Raman spectrum characteristic of type 1 copper of blue copper proteins when excited within its cysteinate → Cu(II) charge-transfer band (620 nm at 298 K, 570 nm at 125 K). The two most intense Raman peaks at 350 and 415 cm^{-1} and the two weaker peaks at 330 and 342 cm^{-1} are assigned to Cu–cysteinate vibrations of one or both of the cysteine ligands. The multiplicity of peaks is indicative of coupling of ν(Cu–S) with ligand modes. The peak at 254 cm^{-1} undergoes a 2-cm^{-1} shift to lower energy in D_2O and is assigned to a Cu–imidazole vibration of the histidine ligand. All of the resonance-enhanced modes display narrow excitation profiles which maximize at ~600 nm (at 15 and 90 K) and appear to coincide with one component of the 570-nm electronic absorption envelope. The peaks in the resonance Raman spectra of Ni(II)- and Fe(III)-substituted alcohol dehydrogenase are very close in frequency and intensity to those of the Cu(II) protein, supporting the view that the protein imposes a tetrahedral structure at the catalytic metal site with at least one short metal–S(Cys) bond. Binding of ligands such as pyrazole, imidazole, β-mercaptoethanol, and cyanide to Cu^{II}-LADH induces 3–20-cm^{-1} shifts in the four main Cu–cysteinate vibrations and causes a substantial decrease in the intensities of the two high-energy Cu–cysteinate peaks. Low-temperature electronic spectra of these binary complexes show absorption maxima close to 500 nm which are significantly blue-shifted from the 570-nm maximum in the low-temperature spectrum of Cu^{II}-LADH. These spectral alterations can be interpreted in terms of a distortion toward a tetragonal geometry at the metal site. In contrast, the binary NADH complex and the ternary NAD^+/pyrazole complex both exhibit intensity increases in the two high-frequency Cu–cysteinate modes as well as a rich set of overtone and combination bands. These resonance Raman features are new signatures of tetrahedral coordination which correlate well with optical and EPR indicators of type 1 copper sites. The Cu^{II}-LADH/NADH complex further resembles the blue copper proteins in that the Cu–cysteinate peaks are strongly affected by deuteration but differs in that there are deuterium-induced alterations in intensities as well as frequencies. It is proposed that these deuterium isotope effects are due to hydrogen bonding of the cysteinate ligand sulfur atoms to suitable protein donors, as is typical of metal–sulfur centers in other metalloproteins.

Liver alcohol dehydrogenase (LADH) is an enzyme which depends on an active-site zinc ion for its catalytic activity. The X-ray crystal structure of the enzyme shows that this zinc ion is tetrahedrally coordinated to two protein cysteinates, one histidine, and a water molecule (Figure 1). Under certain conditions the catalytic zinc ion can be selectively removed from the enzyme, leaving a second structural zinc ion intact. Any one of a number of different metal ions can then be substituted into the catalytic site. Although the enzymatic activity varies in the order Zn(II), Co(II), Ni(II) > Cd(II) ≫ Cu(II), Fe(III), crystallographic and spectroscopic studies indicate that the tetrahedral nature of the coordination site is relatively unchanged upon metal substitution.[3] The close similarity of the X-ray structures for the Co(II), Cd(II), and Zn(II) sites, and even the metal-free site in the apoenzyme,[3] suggests that the protein provides a fairly rigid framework for the ligands and, thereby, strongly influences the metal ion coordination geometry. The enforced tetrahedral character of the metal site in alcohol dehydrogenase is reminiscent of the blue copper protein plastocyanin, which also retains its pseudotetrahedral ligand arrangement at the copper binding site after the copper has been removed or replaced with Hg(II).[4] In plastocyanin and azurins, the Cu(II) ion is trigonally coordinated to two protein histidines and one cysteinate, with a methionine sulfur (plastocyanin) or a methionine sulfur plus a carbonyl oxygen (azurins) at longer distances.[5] Despite the different ligand set, Cu^{II}-LADH also exhibits the unusual electronic and EPR spectral properties[6,7] which are the trademark of the blue copper proteins.[8]

The cupric site of the blue copper proteins has been shown to produce strongly resonance-enhanced Raman spectra.[9] The interpretation of these spectra has proven to be difficult because of the multiplicity of bands in the metal–ligand vibration region, the anomalously high frequencies of these bands, and the variation in both frequency and intensity of the bands among the different blue copper proteins.[10] In view of the importance of proteins with blue copper centers in biochemical systems,[11] an interpretation of the resonance Raman (RR) spectra in terms of the coordination environment of the copper ion is highly desirable. Different approaches have been applied to this end: (1) normal coordinate analyses have been performed which show that the multiplicity of bands can be accounted for by the coupling of Cu–cysteinate and Cu–imidazole vibrational modes;[12a,13] (ii) atom and isotope

(1) (a) Universität des Saarlandes. Present address: Center for Biochemical and Biophysical Sciences and Medicine, Harvard Medical School, Boston, MA 02115. (b) Oregon Graduate Center.

(2) Eklund, H.; Brändén, C.-I. In *Zinc Enzymes*; Spiro, T. G., Ed.; Wiley: New York, 1983; Chapter 4.

(3) (a) Zeppezauer, M.; Andersson, I.; Dietrich, H.; Gerber, M.; Maret, W.; Schneider, G.; Schneider-Bernlöhr, H. *J. Mol. Catal.* **1984**, *23*, 377. (b) Schneider, G.; Eklund, H.; Cedergren-Zeppezauer, E.; Zeppezauer, M. *Proc. Natl. Acad. Sci. U.S.A.* **1983**, *80*, 5289. (c) Schneider, G.; Cedergren-Zeppezauer, E.; Eklund, H.; Knight, S.; Zeppezauer, M. *Biochemistry* **1985**, *24*, 7503.

(4) (a) Garrett, T. P. J.; Clingeleffer, D. J.; Guss, J. M.; Rogers, S. J.; Freeman, H. C. *J. Biol. Chem.* **1984**, *259*, 2822. (b) Church, W. B.; Guss, J. M.; Potter, J. J.; Freeman, H. C. *J. Biol. Chem.* **1986**, *261*, 234.

(5) (a) Guss, J. M.; Freeman, H. C. *J. Mol. Biol.* **1983**, *169*, 521. (b) Adman, E. T.; Jensen, L. H. *Isr. J. Chem.* **1981**, *21*, 8. (c) Norris, G. E.; Anderson, B. F.; Baker, E. N. *J. Mol. Biol.* **1983**, *165*, 501. (d) Adman, E. T. In *Metalloproteins*; Harrison, P. M., Ed.; Verlag Chemie: Weinheim, 1985; Part 1, Chapter 1. (e) Norris, G. E.; Anderson, B. F.; Baker, E. N. *J. Am. Chem. Soc.* **1986**, *108*, 2784.

(6) Maret, W.; Dietrich, H.; Ruf, H.-H.; Zeppezauer, M. *J. Inorg. Biochem.* **1980**, *12*, 241.

(7) Maret, W.; Zeppezauer, M.; Desideri, A.; Morpurgo, L.; Rotilio, G. *Biochim. Biophys. Acta* **1983**, *743*, 200.

(8) Solomon, E. I.; Penfield, K. W.; Wilcox, D. E. *Struct. Bonding (Berlin)* **1983**, *53*, 1.

(9) Siiman, O.; Young, N. M.; Carey, P. R. *J. Am. Chem. Soc.* **1974**, *96*, 5583.

(10) Loehr, T. M.; Sanders-Loehr, J. In *Copper Proteins and Copper Enzymes*; Lontie, R., Ed.; CRC: Boca Raton, 1984; Vol. 1, Chapter 5.

(11) Farver, O.; Pecht, I. ref 10, Chapter 7.

0002-7863/86/1508-6351$01.50/0

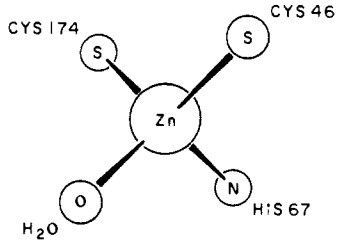

Figure 1. Structure of the catalytic zinc site in native alcohol dehydrogenase based on X-ray diffraction data at 2.4-Å resolution.[2] The ranges of bond lengths and angles in the orthorhombic, open conformation are Zn-S, 2.1-2.3 Å; Zn-N,O, 2.1-2.2 Å, L-Zn-L', 100-127°.

substitution experiments have been undertaken to assign vibrational modes to specific ligands;[12-14] and (iii) spectra have been recorded at cryogenic temperatures to achieve greater spectral resolution.[14,15] We have chosen to investigate the properties of Cu(II)-substituted LADH which exhibits a RR spectrum typical of type 1 copper proteins[16] and which is also amenable to alteration in metal-ligands and coordination geometry.

The dominant features in the RR spectrum of Cu^{II}-LADH are a set of bands between 350 and 450 cm^{-1} which have been ascribed to coupled Cu-S(Cys) and Cu-N(His) vibrational modes.[16] The high energy of these bands is believed to arise from the coordination geometry imposed by the protein on the copper site with at least one short Cu-S(Cys) bond (<2.2 Å). Since the active-site metal ion in LADH interacts with various molecules that are substrates and inhibitors of the native enzyme as well as being influenced by the binding of the coenzymes NAD^+ and NADH, the metal center can be studied in a number of different states. In the present work, we have extended our earlier findings to include additional Cu^{II}-LADH complexes with inhibitor molecules and coenzymes and to obtain new spectroscopic criteria as a measure of the coordination geometry of the catalytic metal center. We propose hydrogen-bonding interactions between the protein and the sulfur ligands to account for anomalous deuterium isotope effects.

Experimental Section

Materials and Methods. Horse liver alcohol dehydrogenase (EC 1.1.1.1), NAD^+ (Li salt), and NADH (grade I) were obtained from Boehringer-Mannheim. Unless otherwise stated, protein samples were dissolved in TES/K^+ buffer composed of 33 mM 2-[tris(hydroxymethyl)methylamino]-1-ethanesulfonic acid and 0.5 M KCl at pH 7.0. N1,N3-labeled imidazole (99% ^{15}N) was prepared by Isotec, Dayton, OH, and its ^{15}N content was verified by mass spectroscopy. D_2O (99.7%) was purchased from Merck Sharp & Dohme or Sigma, and $H_2{}^{18}O$ (95-99%) was obtained from Monsanto. Cupric oxide containing ^{63}Cu (99.9%) or ^{65}Cu (99.7%) (Oak Ridge National Laboratory) was converted to the bromide salt by treatment with HBr.[17] The ligand $HSC(CH_3)_2CH_2NH_2 \cdot HCl$ was the gift of Dr. Harvey J. Schugar. The $Co^{II}[SC(CH_3)_2CH_2NH_2]_2$ complex was prepared according to the method of Mastropaolo et al.[18] Raman spectra of the solid cobalt complex were obtained at 90 K on an anaerobic sample mixed with Na_2SO_4 and sealed in a glass capillary.

The removal of Zn(II) from the catalytic (c) sites of LADH and reconstitution with Cu(II), Ni(II), or Co(II) was performed on protein crystals in 20% (v/v) *tert*-butyl alcohol in buffer as described previously.[6,19] In these preparations two zinc atoms remain in the noncatalytic (n) metal sites to yield $M(c)_2Zn(n)_2$LADH. Crystals of these metal-substituted enzymes were dissolved anaerobically in TES/K^+ buffer, and each solution was frozen in liquid nitrogen. The Fe(III)-substituted species was prepared as follows. Crystalline enzyme lacking catalytic Zn(II), i.e., $H_4Zn(n)_2$LADH, was incubated anaerobically with a 20-fold molar excess of ferrous ammonium sulfate, 80-fold excess of ethylenediamine, and 160-fold excess of ascorbate in TES/K^+ buffer plus 20% (v/v) *tert*-butyl alcohol (pH 7.2) for 5 days. The sample was then dialyzed against TES/K^+/*tert*-butyl alcohol with two to three changes to remove excess iron, ethylenediamine, and ascorbate. The crystals of Fe^{II}-LADH were dissolved in TES buffer with 0.15 M Na_2SO_4 in place of KCl and 8 mM $(NH_4)_2S_2O_8$ as an oxidant.

Preparation of Cu^{II}-LADH with ^{63}Cu or ^{65}Cu was accomplished by the addition of $CuBr_2$ to a crystalline suspension of $H_4Zn(n)_2$LADH in 33 mM TES/K^+ (pH 7.3) and 20% v/v *tert*-butyl alcohol, as described previously.[6,19a] Deuterium isotope exchange was performed by dialyzing a crystalline suspension of Cu^{II}-LADH (40 mg) at 4 °C against three 40-mL aliquots of 33 mM TES (pH 7) in D_2O and 20% v/v *tert*-butyl alcohol for a total of 3 days. The protein was then dissolved in TES/K^+ buffer in D_2O and immediately frozen. Samples were ~90% in D_2O. For $H_2{}^{18}O$ experiments, Cu^{II}-LADH crystals from a 24-mg suspension were equilibrated for 12 h in $H_2{}^{18}O$ buffer (0.85 mL) plus *tert*-butyl alcohol (0.15 mL), then dissolved in $H_2{}^{18}O$ buffer (0.2 mL), and immediately frozen. Samples were at least 80% in $H_2{}^{18}O$.

The protein samples were thawed just prior to Raman experiments, treated with coenzymes or ligands, transferred to capillary tubes, and frozen in liquid nitrogen, all under a nitrogen atmosphere. Protein concentrations were determined from ϵ_{280} = 18 000 M^{-1} cm^{-1} per 40 000 M_r monomer. The metal contents of the metal-substituted LADH samples were estimated from their respective room-temperature absorptivities (in M^{-1} cm^{-1}) per metal ion: ϵ_{620} = 4000 for Cu^{II}-LADH, ϵ_{407} = 3500 for Ni^{II}-LADH, and ϵ_{525} = 1500 for Fe^{III}-LADH.

Raman Spectroscopy. Raman data were collected as described previously[16] on a computer-interfaced Jarrell-Ash spectrophotometer equipped with Spectra-Physics Model 164 Ar and Kr lasers, an RCA C31034A photomultiplier tube, and on Ortec Model 9302 amplifier-discriminator. For spectra at 90 or 278 K, samples were held in capillaries in a cold-finger Dewar.[20] For spectra at 15 K, samples were pipetted directly onto a gold-plated cold finger of a closed-cycle helium refrigerator (Air Products) which was then cooled to ~225 K under nitrogen, evacuated, and then cooled to 15 K. All spectra were obtained in a backscattering geometry. For comparison of isotopically substituted samples, spectra were run consecutively by using identical instrumental conditions, and spectral shifts were verified from computer-generated difference spectra. Although this technique gives reproducible results for frequency shifts ≥ 1 cm^{-1}, absolute frequencies are accurate to only ±1 cm^{-1}.

Low-Temperature Optical Spectroscopy. Spectra were recorded with a Hitachi/Perkin-Elmer 556 dual-wavelength/double-beam spectrophotometer. Samples were held in a 2-mm-path length cryogenic cell cooled with liquid nitrogen.

Results

Cu^{II}-LADH. The resonance Raman spectrum of Cu^{II}-LADH is dominated by a peak at 415 cm^{-1} and a broader, asymmetric band at ~350 cm^{-1} which has components at 350, 342, and 330 cm^{-1} (Figure 2B). Additional peaks are observed at 311, 254, and 198 cm^{-1}. As an aid to assigning these peaks we examined the RR spectrum of the protein in D_2O. Deuteration has been particularly useful in distinguishing between the spectral contributions of histidine and cysteinate ligands because only the imidazole group has exchangeable protons. In the case of Cu^{II}-LADH, the peaks at 311, 254, and 198 cm^{-1} all shift to lower energy when the protein is equilibrated with D_2O (Figure 2A, Table I), whereas the peaks at 415 and 342 cm^{-1} appear mainly to undergo changes in relative intensities. These changes are more readily apparent in the difference spectrum (D_2O minus H_2O) shown in Figure 2C. The peaks of the H_2O sample at 311, 254, 227 (ice), and 198 cm^{-1} have all decreased in intensity in D_2O with corresponding increases in their intensities at lower energies;

(12) (a) Thamann, T. J.; Frank, P.; Willis, L. J.; Loehr, T. M. *Proc. Natl. Acad. Sci. U.S.A.* **1982**, *79*, 6396. (b) Ainscough, E. W.; Bingham, A. G.; Brodie, A. M.; Ellis, W. R.; Gray, H. B.; Loehr, T. M.; Plowman, J. E.; Norris, G. E.; Baker, E. N. *Biochemistry*, in press.

(13) Nestor, L.; Larrabee, J. A.; Woolery, G.; Reinhammar, B.; Spiro, T. G. *Biochemistry* **1984**, *23*, 1084.

(14) Blair, D. F.; Campbell, G. W.; Schoonover, J. R.; Chan, S. I.; Gray, H. B.; Malmström, B. G.; Pecht, I.; Swanson, B. I.; Woodruff, W. H.; Cho, W. K.; English, A. M.; Fry, H. A.; Lum, V.; Norton, K. A. *J. Am. Chem. Soc.* **1985**, *107*, 5755.

(15) Woodruff, W. H.; Norton, K. A.; Swanson, B. I.; Fry, H. A. *Proc. Natl. Acad. Sci. U.S.A.* **1984**, *81*, 1263.

(16) Maret, W.; Zeppezauer, M.; Sanders-Loehr, J.; Loehr, T. M. *Biochemistry* **1983**, *22*, 3202.

(17) Brauer, G. *Handbook of Preparative Inorganic Chemistry*; Academic: New York, 1965.

(18) Mastropaolo, D.; Thich, J. A.; Potenza, J. A.; Schugar, H. J. *J. Am. Chem. Soc.* **1977**, *99*, 424.

(19) (a) Maret, W.; Andersson, I.; Dietrich, H.; Schneider-Bernlöhr, H.; Einarsson, R.; Zeppezauer, M. *Eur. J. Biochem.* **1979**, *98*, 501. (b) Dietrich, H.; Maret, W.; Kozlowski, H.; Zeppezauer, M. *J. Inorg. Biochem.* **1981**, *14*, 297.

(20) Sjöberg, B.-M.; Loehr, T. M.; Sanders-Loehr, J. *Biochemistry* **1982**, *21*, 96.

Table I. Resonance Raman Vibrational Frequencies (cm^{-1}) for Metal-Substituted Alcohol Dehydrogenase and Blue Copper Proteins[a]

Cu^{II}-LADH	Ni^{II}-LADH	Fe^{III}-LADH	azurin[b]	stellacyanin[b,c]	laccase[c]	assignment[b,c]
198 m (*1*)			188 w	180 w	202 w	
254 m (*2*)	257 m		287 w (*5*)	275 w (*2*) [*0*]	265 w[d]	ν(Cu-Im)
311 m (*4*)[e]	312 m	309 w	308 w			
330 m			333 w	335 w	333 w	
342 m			348 w (*2*) [*0*]		346 w	
350 s	350 s	357 s	373 m (*1*) [*1*]	348 m (*2*) [*2*]	381 s (*1*) [*1*]	
378 w	375 w	387 m	409 s (*1*) [*1*]	374 w (*2*) [*2*]	405 s (*1*) [*1*]	ν(Cu-S) + δ(Cys)
415 s (*0*)	414 s	428 s	428 m (*1*) [*0*]	386 s (*2*) [*2*]	420 s (*0*) [*0*]	

[a] Metal-substituted LADH samples at 90 K; *P. aeruginosa* azurin at 12 and 25 K; *Rhus vernicifera* stellacyanin at 12, 77, and 300 K; *R. vernicifera* laccase at 77 K. Peak intensities denoted by s = strong, m = medium, w = weak. Isotope shifts to lower frequency upon substituting D_2O for H_2O denoted by (ΔD); ^{65}Cu for ^{63}Cu denoted by [ΔCu]. Magnitude of isotope shift rounded off to nearest whole number. [b] References 14 and 15. [c] Reference 13. [d] This broad band did not exhibit a clear deuterium isotope shift and may contain a Cu-S-C bending mode in addition to the Cu-Im stretch. [e] Deuterium isotope shift determined in samples at 278 K to eliminate interference of ice mode at 308 cm^{-1}.

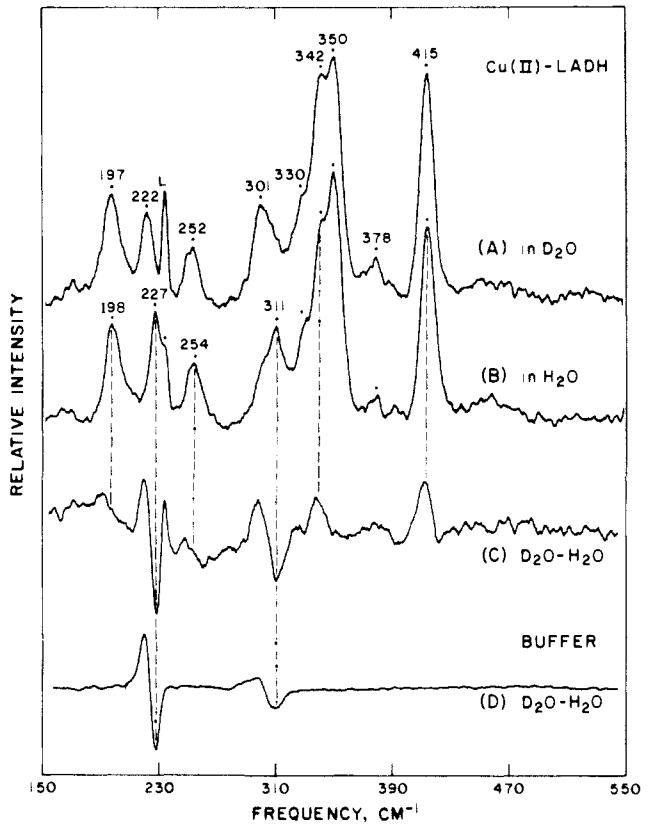

Figure 2. Resonance Raman spectrum of Cu(II)-substituted alcohol dehydrogenase at 90 K. (A) Cu^{II}-LADH in D_2O, 2.3 mM in protein, 1.2 mol of Cu/dimer. Spectrum obtained with 647.1-nm excitation, 1 cm^{-1}/s scan rate, 5-cm^{-1} resolution, ~100-mW laser power at the sample Dewar, sum of 19 scans. L denotes a laser plasma line. (B) Cu^{II}-LADH in H_2O, 2.2 mM in protein, 1.3 mol of Cu/dimer, in 33 mM TES, 0.15 M Na_2SO_4 (pH 7.0). Conditions as in (A), sum of 16 scans. Unlabeled peaks (●) in the H_2O spectrum are at the same frequencies as in the D_2O spectrum. (C) Computer-generated difference spectrum of (A) minus (B). (D) Computer-generated difference spectrum of D_2O buffer minus H_2O buffer. Spectra obtained with 514.5-nm excitation, five scans, other conditions as in (A).

these shifts are indicative of isotope effects. In contrast, the H_2O sample peaks at 415 and 342 cm^{-1} have increased in intensity in D_2O (possibly due to peak sharpening), but with no detectable shift in frequency.

The Cu^{II}-LADH feature at 254 cm^{-1} is in the expected location for a Cu-imidazole vibrational mode. This identification is supported by the 2-cm^{-1} shift in the deuterated protein (Figure 2). Similar deuterium-sensitive vibrations are observed at 245 cm^{-1} in $Cu(ImH)_4Cl_2$,[21] at 267 cm^{-1} in hemocyanin,[21] at 287 cm^{-1} in azurin,[14] and at 274 cm^{-1} in stellacyanin.[13,14] A 2-cm^{-1} shift in this peak has been considered to be indicative of exchange of both the nitrogen (N1 or N3) and C2 protons of imidazole.[13,21] However, the magnitude of the isotope shift does not correlate well with the number of exchangeable hydrogens per histidine. Thus, in the spectrum of azurin obtained at cryogenic temp., the Cu-imidazole frequency decreases by 5 cm^{-1} in D_2O.[14] In the present case, Cu^{II}-LADH shows a 2-cm^{-1} shift in D_2O, although nuclear magnetic resonance studies of Co^{II}-LADH indicate that only the N1 proton of the imidazole ligand exchanges with deuterium.[22]

The effect of deuterium isotope exchange on the peak at 311 cm^{-1} is complicated by the presence of a deuterium-sensitive ice mode in this vicinity. Figure 2D shows that frozen buffer at 90 K exhibits ice translational vibrations[23] at 227 and 308 cm^{-1}, which shift to 222 and 299 cm^{-1} in D_2O. The 308-cm^{-1} peak in ice is typically 20–30% of the intensity of the 227-cm^{-1} peak. Although this same set of peaks is clearly present in the protein difference spectrum (Figure 2C), the intensity in the 311–301-cm^{-1} region relative to the 225–222-cm^{-1} region is about twice that of the buffer alone. This implies that the protein contains a deuterium-sensitive component near 310 cm^{-1}. The spectrum of Cu^{II}-LADH in solution at 278 K also reveals a significant feature near 310 cm^{-1} that shifts −4 cm^{-1} in D_2O, further corroborating that this feature is indeed related to deuteration of the protein.

One possible assignment for the 311-cm^{-1} peak in Cu^{II}-LADH is to a vibration of the metal-bound water molecule which has been detected in the crystal structures of Zn^{II}-LADH,[2] Co^{II}-LADH,[3b] and Cd^{II}-LADH[3c] and implicated for Cu^{II}-LADH by NMR relaxation studies.[24] However, we were unable to obtain supporting evidence for such an assignment with $H_2{}^{18}O$ solvent. Low-temperature spectra in $H_2{}^{18}O$ showed shifts in the 311- and 227-cm^{-1} ice peaks similar to those observed in D_2O (Figure 2A), but difference spectra of the Cu^{II}-LADH samples ($H_2{}^{18}O$ minus $H_2{}^{16}O$) were essentially indistinguishable from those of the buffer alone. Spectra obtained on solution samples in $H_2{}^{18}O$ at 278 K also revealed no significant changes in the 310-cm^{-1} region relative to those in $H_2{}^{16}O$.

The peaks at 350 and 415 cm^{-1} in Cu^{II}-LADH are typical of the two strong features generally observed at 350–380 and 385–420 cm^{-1} in the RR spectra of the blue copper proteins (Table I). The intensity of these peaks and the fact that they are in resonance with the ~600-nm σS(Cys) → Cu(II) charge-transfer band[8] have led to their assignment as Cu-S(Cys) vibrations.[12-14] The high energies of these vibrations (relative to the metal–sulfur stretch of model compounds)[10] can be explained by the presence of a short Cu-S bond (~2.1 Å) in each of the proteins. However, the multiplicity of peaks in this region and their smaller-than-expected Cu-isotope dependence (Table I) have led to the proposal that these peaks represent substantial admixing of cysteinate ligand modes such as δ(S-C-C) with the Cu-S stretch.[13-15] By analogy, the two intense peaks at 350 and 415 cm^{-1} in Cu^{II}-LADH and

(21) Larrabee, J. A.; Spiro, T. G. *J. Am. Chem. Soc.* **1980**, *102*, 4217.

(22) Bertini, I.; Gerber, M.; Lanini, G.; Luchinat, C.; Maret, W.; Rawer, S.; Zeppezauer, M. *J. Am. Chem. Soc.* **1984**, *106*, 1826.

(23) Whalley, E. In *The Hydrogen Bond*; Schuster, P., Zundel, G., Sandorfy, C., Eds.; North-Holland: Amsterdam, 1976; Vol. III, p 1425.

(24) Andersson, I.; Maret, W.; Zeppezauer, M.; Brown, R. D., III; Koenig, S. H. *Biochemistry* **1981**, *20*, 3424.

Table II. Resonance Raman, Visible, and EPR Spectral Data for Binary Complexes of Cu^{II}-LADH with Ligands

		Cu-LADH plus				
	NADH	Cu-LADH only	pyrazole	imidazole	$HSCH_2CH_2OH$	cyanide
RR vibrational modes, cm^{-1} [a]						
Cu–X	200	198	198	201	201	202
Cu–His	262	254				
Cu–X	314	311	301	306	305	306
Cu–Cys 1	330	330	322	325	323	
Cu–Cys 2	340	342	337	336	335	341
Cu–Cys 3	357	350	367	364	362	370
Cu–Cys 4	419	415	410	411	408	412
relative intensities of Raman modes[b]						
Cu–Cys (3,4)/Cu–Cys (1,2)	10	2.5	0.7	0.7	0.8	
absorption maxima in nm[c]						
S → Cu(II) CT	690	570	505	480	500	485
EPR parameters[d]						
$A_\parallel \times 10^4$ in cm^{-1}	<30	50	115	127	107	133

[a] Cu–L and ligand vibrations making major contribution to a particular RR mode at 90 K. [b] Calculated from the total intensity of the Cu–Cys 3 and Cu–Cys 4 vibrations divided by the total intensity of the Cu–Cys 1 and Cu–Cys 2 vibrations. [c] Data obtained at 77 K. Values for Cu^{II}-LADH ± NADH from ref 16. Values for binary ligand complexes from present work. [d] Data at 100 K from ref 7 and 27.

probably the weaker features at 330 and 342 cm^{-1} can be assigned as combinations of the Cu–S vibration with ligand deformation modes. These spectra also show far less Cu-isotope dependence than the 3-cm^{-1} shift expected[13] for a pure Cu–S vibration with ^{65}Cu replacing ^{63}Cu. No significant spectral shifts are observed in Cu^{II}-LADH when the metal at natural abundance (63.5 amu) is replaced by ^{65}Cu, indicating that any shifts are less than 1 cm^{-1} in magnitude.

The electronic absorption spectrum of copper-substituted LADH exhibits an intense band in the visible region similar to that of the blue copper proteins. It differs, however, in that the absorption envelope is more clearly composed of multiple electronic transitions and that the relative intensities and energies of these transitions vary with temperature. The room-temperature absorption maximum at 620 nm shifts successively to higher energy as the temperature is lowered; it is near 600 nm at 264 K and near 570 nm at 125 K (Figure 3A). Despite the marked changes in the optical spectrum with temperature, the resonance Raman spectrum is essentially unaltered between 15 and 278 K. This indicates that little or no structural rearrangement of the copper center accompanies these absorption spectral changes. As judged from the excitation profile, the cysteine → copper charge-transfer transition responsible for resonance enhancement is localized within a narrow region of the absorption envelope (Figure 3B). For Cu^{II}-LADH at 15 K in D_2O the protein vibrational modes at 252, 307, 349, and 414 cm^{-1} as well as the peaks at 199, 330, 341, and 377 cm^{-1} (data not shown) all have a sharp excitation profile that maximizes at 600 nm. A similar enhancement maximum is observed at 90 K. The appearance of a single enhancement peak despite the fact that Cu^{II}-LADH contains two cysteine ligands suggests either that the two $\sigma S \rightarrow Cu(II)$ charge-transfer transitions are close in energy or that only one of the copper–cysteinates generates the observed RR spectrum. It is of interest in this context that the resonance Raman spectrum of Cu^{II}-LADH is closely matched (Table I) in peak number, frequencies, and intensities with the spectra of blue copper proteins containing only a single cysteine ligand.

Binary Complexes with Inhibitors. Pyrazole and imidazole are competitive inhibitors of native alcohol dehydrogenase which appear to occupy the same position as substrate in the coordination sphere of the active-site metal ion.[2,25] Direct metal binding of imidazole and pyrazole nitrogen atoms in binary complexes of Zn^{II}-LADH has been observed by X-ray crystallography.[26] In the case of Cu^{II}-LADH, pyrazole and imidazole coordination is evident from the appearance of additional nitrogen hyperfine lines in the $g_\perp$ region of the EPR spectrum.[6] Mercaptoethanol and cyanide are believed to form similar complexes to those with pyrazole and imidazole since all four yield a corresponding increase in the $A_\parallel$ value of the Cu(II) EPR signal: from 50×10^{-4} cm^{-1}

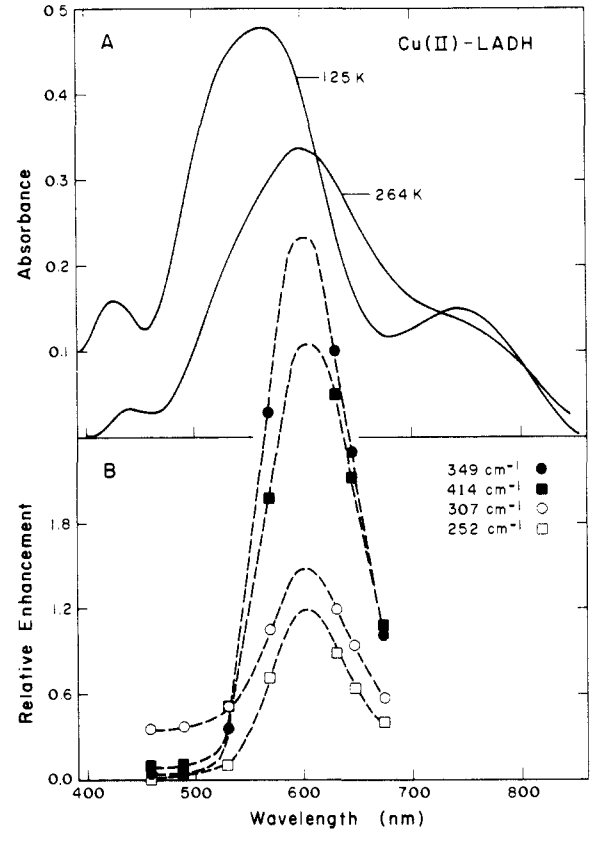

Figure 3. Absorption spectra and resonance Raman enhancement profiles for Cu^{II}-LADH. (A) Absorption spectra recorded at 264 and 125 K for a sample 0.8 mM in protein in 0.1 M BTP (1,3-bis[tris(hydroxymethyl)methylamino]propane), 0.15 M Na_2SO_4 (pH 8.5). (B) Enhancement profiles for vibrations at 252, 307, 414, and 349 cm^{-1} for a sample of ^{65}Cu-substituted LADH, 1.1 mM in protein in 33 mM TES, 0.15 M Na_2SO_4 in D_2O (pD 7.4). All Raman spectra were obtained on a single sample at 15 K. Enhancement was measured as the height of the Raman peak relative to the height of the ice peak at 225 cm^{-1}. Sample integrity, as monitored by intensity with 514.5-nm excitation, was unaltered during the 12-h period in which data were collected. Peak positions are somewhat altered relative to those shown in Figure 2A due to the decrease in temperature, but the relative peak intensities obtained with 647.1-nm excitation are unchanged at 15 K. The contribution of the ice mode to the enhancement of the 307-cm^{-1} peak can be seen in the 450–520-nm region where its intensity is independent of excitation wavelength.

(25) Zeppezauer, M. In *The Coordination Chemistry of Metalloenzymes*; Bertini, I., Drago, R. S., Luchinat, C., Eds.; Reidel: Dordrecht, 1983; p 99.
(26) (a) Eklund, H.; Samama, J.-P.; Wallén, L. *Biochemistry* **1982**, *21*, 4858. (b) Boiwe, T.; Brändén, C.-I. *Eur. J. Biochem.* **1977**, *77*, 173.
(27) Maret, W.; Zeppezauer, M.; Desideri, A.; Morpurgo, L.; Rotilio, G. *FEBS Lett.* **1981**, *136*, 72.

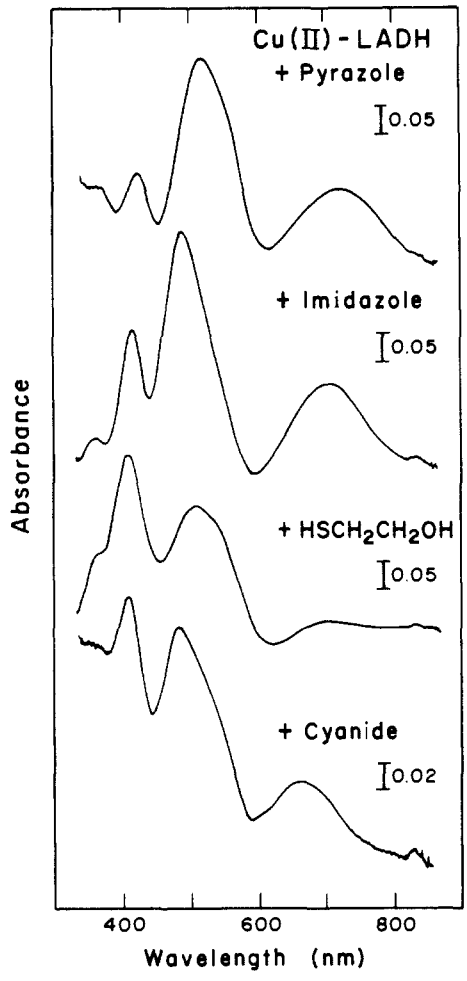

Figure 4. Absorption spectra of binary complexes of Cu^{II}-LADH with pyrazole, imidazole, β-mercaptoethanol, and cyanide at ~120 K. Pyrazole complex: 0.67 mM in protein, 62 mM in pyrazole, 0.1 M BTP, 0.15 M Na_2SO_4 (pH 8.5). Imidazole complex: 0.67 mM in protein, 67 mM in imidazole, 33 mM TES, 0.15 M Na_2SO_4 (pH 7.0). β-Mercaptoethanol complex: 0.67 mM in protein, 1.4 mM in β-mercaptoethanol, 33 mM TES/SO_4 (pH 7.0). Cyanide complex: 0.34 mM in protein, 2.5 mM in cyanide, 33 mM TES/SO_4 (pH 7.0).

in Cu^{II}-LADH to 107–133 × 10^{-4} cm^{-1} in the binary ligand complexes (Table II). In addition, in all four cases the cysteinate sulfur-to-copper charge-transfer band in the low-temperature optical spectrum shifts to higher energy: from 570 nm in Cu^{II}-LADH to 485–505 nm in the binary ligand complexes (Figure 4 and Table II). Studies on other blue copper proteins and model compounds have led to the conclusion that larger $A_{\parallel}$ values and higher energy charge-transfer bands are indicative of a departure from near-tetrahedral coordination geometry.[8,28] A similar structural alteration is presumably responsible for the analogous changes in the spectra of the binary complexes of Cu^{II}-LADH.

The pyrazole complex of Cu^{II}-LADH exhibits a set of RR vibrational modes analogous to those of the ligand-free protein, but with some interesting shifts in frequencies and intensities (Figure 5). The 254-cm^{-1} Cu–histidine mode of Cu^{II}-LADH is less marked in the spectrum shown for the pyrazole adduct, but a peak near 250 cm^{-1} has been observed in other spectra of this complex. The peaks at 311, 330, 342, 350, and 415 cm^{-1} in Cu^{II}-LADH are represented by peaks at 301, 322, 337, 367, and 410 cm^{-1} in Cu^{II}-LADH plus pyrazole. In addition to the 5- and 17-cm^{-1} shifts in frequency in the binary complex, the peaks at

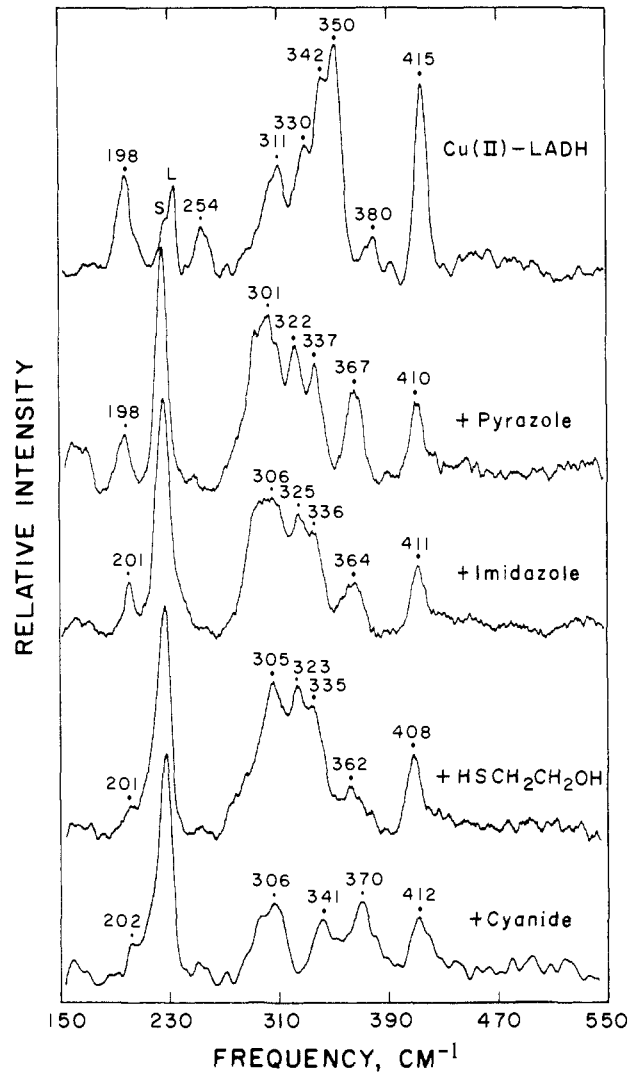

Figure 5. Resonance Raman spectra of binary complexes of Cu^{II}-LADH with pyrazole, imidazole, β-mercaptoethanol, and cyanide at 90 K. Conditions as in Figure 2, unless otherwise noted. Cu^{II}-LADH: 2.4 mM in protein, 1.5 mol of Cu/dimer, 7 scans. Pyrazole complex: 2.0 mM in protein, 1.3 mol of Cu/dimer, 0.1 M in pyrazole, 514.5 nm, 100 mW, 16 scans. Imidazole complex: 2.0 mM in protein, 0.1 M in imidazole, 514.5 nm, 50 mW, 7.5-cm^{-1} resolution, 2 cm^{-1}/s scan rate, 137 scans. β-Mercaptoethanol complex: 2.0 mM in protein, 4.7 mM in β-mercaptoethanol, 514.5 nm, 25 mW, 7.5-cm^{-1} resolution, 2 cm^{-1}/s scan rate, 62 scans. Cyanide complex: 1.8 mM in protein, 1.1 mol of Cu/dimer, 2.4 mM in cyanide, 514.5 nm, 50 mW, 7.5-cm^{-1} resolution, 2 cm^{-1}/s scan rate, 22 scans.

367 and 410 cm^{-1} are markedly decreased in intensity relative to the peaks at 322 and 337 cm^{-1}. Upon deuteration, the only Raman band that shifts to lower energy is in the broad 301-cm^{-1} envelope. The difference spectrum (D_2O minus H_2O, data not shown) for the pyrazole complex shows a peak at 296 cm^{-1} and trough at 308 cm^{-1} whose intensities relative to the 222-cm^{-1} peak and 227-cm^{-1} trough of ice are closer to those observed for buffer alone (Figure 2D) than for Cu^{II}-LADH (Figure 2C). Thus, the 301-cm^{-1} feature of the pyrazole complex does not appear to have as much of a deuterium isotope dependence as the 311-cm^{-1} feature in Cu^{II}-LADH. Other similarities between the pyrazole complex and free Cu^{II}-LADH are the $H_2{}^{18}O$ and $H_2{}^{16}O$ difference spectrum (which is identical with that of buffer alone) and the lack of any isotope shifts > 1 cm^{-1} between the ^{63}Cu- and ^{65}Cu-substituted forms.

The binary complexes of Cu^{II}-LADH with imidazole and β-mercaptoethanol exhibit RR spectra which are strikingly similar to those of the pyrazole complex (Figure 5 and Table II). All show the ~200-cm^{-1} peak, are diminished in intensity in the ~250-cm^{-1} histidine peak, have the ~305-cm^{-1} mode as the most intense RR peak in the spectrum, and exhibit a set of *four* vi-

(28) (a) Schugar, H. J. In *Copper Coordination Chemistry: Biochemical and Inorganic Perspectives*; Karlin, K. D., Zubieta, J., Eds.; Adenine: New York, 1983; p 43. (b) Dorfman, J. D.; Bereman, R. D.; Whangbo, M.-H. ref 28a, p 75. (c) Anderson, O. P.; Becher, J.; Frydendahl, H.; Taylor, L. F.; Toftlund, H. *J. Chem. Soc., Chem. Commun.* **1986**, 699.

brations at approximately 325, 335, 365, and 410 cm^{-1}, with the former two (1 and 2) being more intense than the latter two (3 and 4). In these complexes, then, neither the protein histidine ligand nor the exogenous ligand (e.g., pyrazole, imidazole) appears to contribute significantly to the RR spectrum. This observation was verified by preparing the Cu^{II}-LADH imidazole complex from imidazole in which both nitrogens had been substituted with ^{15}N. The RR spectrum of the [^{15}N]imidazole adduct was indistinguishable from that obtained with [^{14}N]imidazole. Thus, peaks 1–4 in the binary complexes must be predominantly vibrations of the bound cysteinates. The cyanide complex of Cu^{II}-LADH (Figure 5 and Table II) yielded a RR spectrum of lower quality. However, with the exception of peak 1 at ~325 cm^{-1}, the pattern of frequencies and intensities is similar to that of the other binary complexes.

The variation in the relative intensities of the four Cu–cysteinate vibrational modes upon ligand binding is particularly striking. The ratio of the peak heights for the two higher energy modes (3 + 4) relative to the two lower energy modes (1 + 2) changes from 2.5 in Cu^{II}-LADH to 0.7–0.8 in the complexes with pyrazole, imidazole, and β-mercaptoethanol (Table II). When different excitation wavelengths were used to obtain the RR spectra, these affected the overall spectral quality but did not alter the intensities of the Raman bands relative to one another. By using the ice mode at 227 cm^{-1} as an intensity standard, we found that the variations in peak ratios are primarily due to the intensities of vibrational modes 3 and 4. Thus, upon formation of the binary complexes, peaks 1 and 2 decrease only slightly relative to the ice mode, while peaks 3 and 4 show ~6-fold decreases in intensity. These changes in resonance enhancement reflect a decrease in the extent of vibrational coupling to the electronic transition and, thereby, signal a change in coordination geometry. The higher energies of the optical absorptions and the larger $A_{\parallel}$ values in the EPR spectra of the binary ligand complexes of Cu^{II}-LADH suggest a loss of tetrahedral character at the metal site; it is likely that the decreased intensities of peaks 3 and 4 are another manifestation of this same structural alteration.

Complexes with Coenzymes. Binding of NADH to Zn^{II}-LADH has been shown by X-ray crystallography to convert the protein from an open to a closed conformation,[2,29] which may be accompanied by small changes in bond distances and angles at the catalytic metal site. The narrowness of the EPR hyperfine splitting ($A_{\parallel} < 30 \times 10^{-4}$ cm^{-1}) and the low energy of the charge-transfer band at 690 nm (Table II) both indicate a more nearly tetrahedral geometry for the copper ion in the NADH complex.[30] The RR spectrum of the binary complex of Cu^{II}-LADH plus NADH (Figure 6A, Table II) shows all of the major features of Cu^{II}-LADH but with some shifts in frequencies and altered intensities, which must be attributed to structural changes induced by coenzyme binding. The cysteine-related vibrations at 358 and 419 cm^{-1} are 4–7 cm^{-1} higher in energy than in Cu^{II}-LADH, indicating a slightly reduced metal–sulfur distance. A similar bond decrease has been suggested for the coenzyme-bound form of Cd(II)-substituted LADH on the basis of perturbed angular correlation spectroscopy.[31] In addition, the 358- and 419-cm^{-1} peaks in Cu^{II}-LADH plus NADH are ~3-fold more intense (relative to the 227-cm^{-1} ice mode) than the corresponding peaks in Cu^{II}-LADH. Thus, in the NADH complex the intensity ratio of the high-energy modes (Cu–Cys 3 + 4) to the low-energy modes (Cu–Cys 1 + 2) has a value of 10 (Table II). The increase in the intensity of peaks 3 and 4 appears to correlate well with the EPR and optical indicators of tetrahedral coordination. In all three of these characteristics, it is the coenzyme-bound form of Cu^{II}-LADH which shows the closest resemblance to the spectroscopic properties of the blue copper proteins.

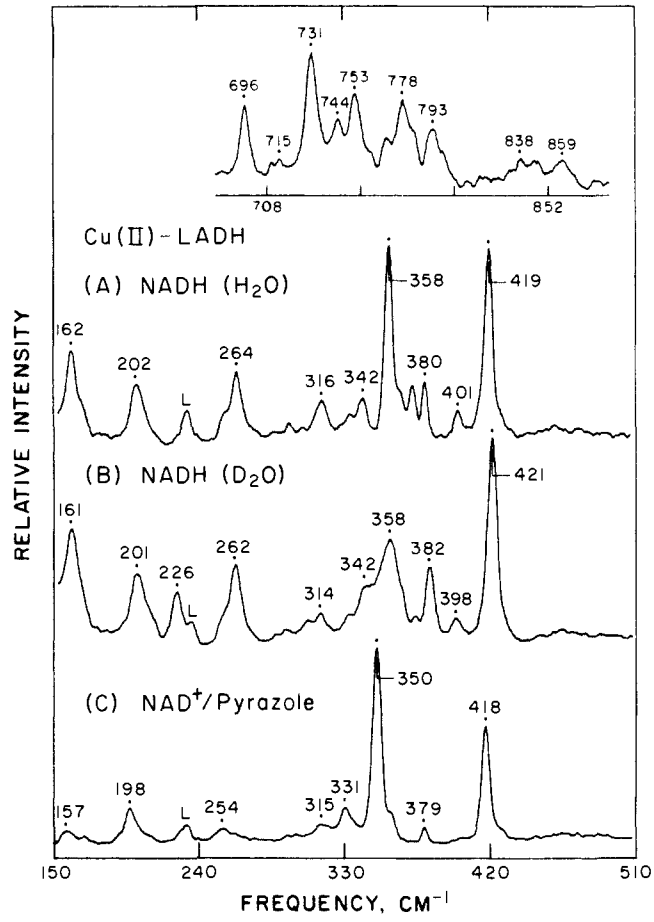

Figure 6. Resonance Raman spectra of Cu^{II}-LADH plus NADH at 15 K. Spectra obtained with ~80-mW laser power at 647.1 nm; sum of 5 scans for each sample. (A) Cu^{II}-LADH + NADH (1.9 mM in protein, 68 mM NAD^+) in H_2O buffer (100 mM BTP, 0.12 M Na_2SO_4, pH 9.0). In 150–510-cm^{-1} range: 3.5-cm^{-1} resolution, 1 cm^{-1}/s. In 650–900-cm^{-1} range: 3.5-cm^{-1} resolution, 0.5 cm^{-1}/s. (B) Cu^{II}-LADH + NADH (0.9 mM in protein, 23 mM NAD^+) in D_2O buffer (130 mM TES, 0.12 M Na_2SO_4, pD 9.0); 5-cm^{-1} resolution, 0.5 cm^{-1}/s. (C) Cu^{II}-LADH + NAD^+ + pyrazole (1.7 mM in protein, 60 mM NAD^+, 84 mM in pyrazole) in H_2O buffer (100 mM BTP, 0.11 M Na_2SO_4, pH 9.0); 3.5-cm^{-1} resolution, 1 cm^{-1}/s. Although the coenzyme was added as NAD^+ in each case, the RR spectra in (A) and (B) are identical with those obtained with NADH; optical spectra and low reactivity toward pyrazole indicate that these complexes have reverted to the NADH state. In (C) the coenzyme and pyrazole were added simultaneously to ensure the NAD^+ state.

An additional feature that the Cu^{II}-LADH/NADH complex shares with the blue copper sites of other proteins is a rich set of resonance-enhanced overtones and combinations (Figure 6, inset). At 15 K, Cu^{II}-LADH plus NADH has fundamentals at 334, 342, 358, 372, 380, 401, 419, 744 (protein mode), and 753 cm^{-1} (C–S stretch), weak ovetones at 715 (2 × 358) and 838 (2 × 419) cm^{-1}, and a rich set of well-resolved combination bands at 696 (342 + 358), 731 (358 + 372), 778 (358 + 419), and 793 cm^{-1} (372 + 419). The multiplicity of overtone and combination bands is considerably greater than in the absence of coenzyme[16] and is similar to that observed in other blue copper sites.[14] The anomalously high intensity of combination bands relative to overtones has also been noted for plastocyanin[15] and fungal laccase.[33] Since the tetrahedral iron–sulfur centers of oxidized rubredoxin and adrenodoxin also give rise to a complex set of overtone and combination bands in their resonance Raman spectra,[32] this may well be a general property of tetrahedral metal–sulfur coordination compounds.

(29) Cedergren-Zeppezauer, E.; Samama, J.-P.; Eklund, H. *Biochemistry* **1982**, *21*, 4895.
(30) Maret, W.; Kozlowski, H., unpublished results.
(31) Andersson, I.; Bauer, R.; Demeter, I. *Inorg. Chim. Acta* **1982**, *67*, 53.
(32) (a) Yachandra, V. K.; Hare, J.; Moura, I.; Spiro, T. G. *J. Am. Chem. Soc.* **1983**, *105*, 6455. (b) Yachandra, V. K.; Hare, J.; Gewirth, A.; Czernuszewicz, R. S.; Kimura, T.; Holm, R. H.; Spiro, T. G. *J. Am. Chem. Soc.* **1983**, *105*, 6462.
(33) Nestor, L.; Reinhammar, B.; Spiro, T. G. *Biochim. Biophys. Acta* **1986**, *869*, 286.

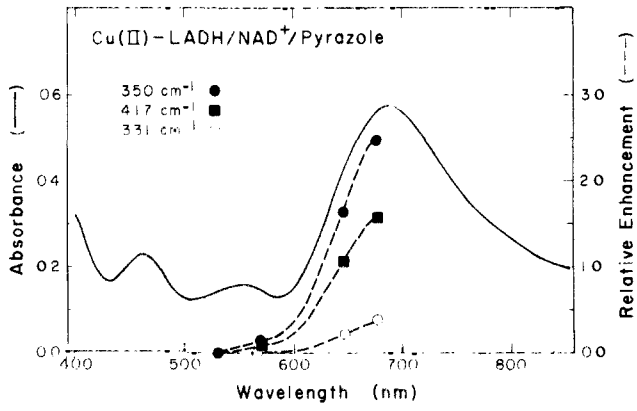

Figure 7. Absorption spectrum and resonance Raman enhancement profiles for the ternary complex of Cu^{II}-LADH with NAD^+ and pyrazole. (—) Absorption spectrum at 123 K for a sample 0.5 mM in protein, 8.5 mM in NAD^+, 33 mM in pyrazole, in 100 mM BTP, 0.04 M Na_2SO_4 (pH 8.5). (---) Enhancement profiles for vibrations at 331, 350, and 417 cm^{-1} for samples as in Figure 6C, diluted 2–5-fold with 0.5 M Na_2SO_4. Raman spectra were obtained at 15 K. Enhancement was measured as the height of the Raman peak relative to the height of the 989-cm^{-1} peak from the 0.5 M Na_2SO_4 internal standard.

As with Cu^{II}-LADH and Cu^{II}-LADH plus pyrazole, isotopic substitution of the copper ion or solvent oxygen has essentially no effect on the Raman spectrum of the NADH complex. Furthermore, none of these species show any Raman spectral changes between pH 7 and 9, indicating that no changes in the ligand ionization state are occurring in this pH range. However, the NADH complex shows unusual behavior upon deuteration (Figure 6B). Whereas the peaks at 202 and 264 cm^{-1} undergo 1- and 2-cm^{-1} shifts to lower energy in D_2O, as observed previously for Cu^{II}-LADH (Table I), the peaks at 358 and 372 cm^{-1} exhibit a dramatic loss in intensity, and the peaks at 380 and 419 cm^{-1} actually shift 2 cm^{-1} to higher energy. These anomalous effects in the 340–420-cm^{-1} region are most likely due to Fermi resonance coupling with a vibrational mode which is strongly affected by deuteration. The deuterium isotope effects in this particular case are much more pronounced than in the blue copper proteins where the peaks above 330 cm^{-1} only decrease in frequency (by 1–2 cm^{-1}) without any alterations in intensity.[13] Although these deuterium isotope effects in the blue copper proteins have previously been described to the admixture of imidazole ring modes with the Cu–S stretch, the extensive changes observed in the Cu^{II}-LADH coenzyme complexes raise the possibility that the deuterium sensitivity in both cases is the result of hydrogen-bonding interactions of the coordinated cysteine sulfurs.

Addition of NAD^+ and pyrazole to Cu^{II}-LADH yields a stable ternary complex. Crystallographic studies of the zinc analogue show that the enzyme is in the closed conformation, with pyrazole directly coordinated to the catalytic metal ion.[26a] The optical spectrum of Cu^{II}-LADH/NAD^+/pyrazole has an intense absorption maximum at 690 nm (Figure 7) which is quite similar to the absorption maximum of the binary Cu^{II}-LADH/NADH complex.[30] The Raman spectrum (Figure 6C) reflects pyrazole coordination on the basis of the ~10-cm^{-1} shifts to lower energy for the peaks at 264 and 358 cm^{-1} and the significant loss of intensity in the peaks at 162, 264, 342, 372, and 401 cm^{-1}. Nevertheless, the spectral pattern of the ternary complex is still very close to that of the binary complex with NADH (Figure 6A). Thus, the copper site appears to remain tetrahedral, a conclusion which is in agreement with EPR spectroscopic data.[30] The behavior of the coenzyme complex (closed conformation) differs considerably from that of the open conformation of Cu^{II}-LADH. In the latter case, binding of pyrazole results in substantial changes in the optical (Figure 4), resonance Raman (Figure 5), and EPR properties (Table II), all of which can be interpreted as a significant distortion toward a more tetragonal geometry.

The Cu^{II}-LADH/NAD^+/pyrazole complex shows a further similarity to the behavior of the blue copper systems in that the resonance Raman enhancement profile for each of its spectral components (Figure 7) appears to coincide with the strong 690-nm absorption band, allowing it to be assigned principally as σS(Cys) → Cu(II) charge transfer. The blue copper proteins azurin[12b] and stellacyanin[34] show a similar correlation between their 610-nm electronic absorption band and their resonance Raman intensities as a function of excitation wavelength. A measure of the extent of resonance enhancement can be obtained from the ratio of the height of a particular peak to that of an internal standard (e.g., $\nu_1(SO_4^{2-})$ at 989 cm^{-1} at 15 K), with each normalized to a molar concentration. The 350-cm^{-1} peak of the Cu^{II}-LADH/NAD^+/pyrazole complex with 676.4-nm excitation has a molar scattering factor of 5400 relative to sulfate. This very strong enhancement of the same order of magnitude as in the blue copper proteins. The 411-cm^{-1} peak of *Alcaligenes denitrificans* azurin, for example, with 647.1-nm excitation has a molar scattering factor of 1300 relative to sulfate.[12b] The greater enhancement of the Cu^{II}-LADH complex is due in part to the closer correspondence of the excitation wavelength with the absorption maximum.

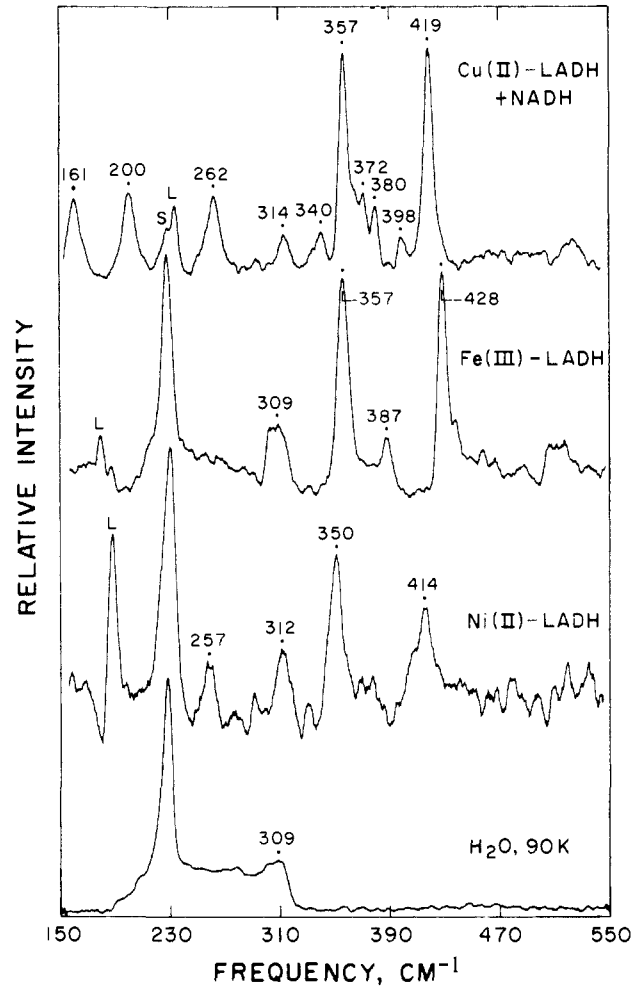

Figure 8. Resonance Raman spectra of Cu^{II}-LADH plus NADH, Fe^{III}-LADH, and Ni^{II}-LADH at 90 K. Conditions as in Figure 2 unless otherwise noted. Cu^{II}-LADH + NADH: 2.4 mM in protein, 1.5 mol of Cu/dimer, 42 mM in NADH, 9 scans. Fe^{III}-LADH: 3.1 mM in protein, 1.1 mol of Fe/dimer, 33 mM TES, 0.15 M Na_2SO_4, 8 mM $(NH_4)_2S_2O_8$ (pH 7.0), 496.5 nm, 50 mW, 27 scans. Ni^{II}-LADH: 3.2 mM in protein, 0.6 mol of Ni/dimer, 406.7 nm, 15 mW, 24 scans. H_2O: 514.5 nm, 100 mW, 3 scans.

Fe^{III}-, Ni^{II}-, and Co^{II}-LADH. Spectroscopic and crystallographic studies of a number of metal-substituted alcohol dehydrogenases have led to the conclusion that the tetrahedral character of the catalytic zinc site is preserved upon metal replacement.[25] The RR spectra of Fe(III)- and Ni(II)-substituted LADH (Figure 8, Table I) provide direct evidence for this viewpoint. Both show

(34) Musci, G.; Desideri, A.; Morpugo, L., Tosi, L. *J. Inorg. Biochem.* **1985**, *23*, 93.

metal–cysteinate vibrations at frequencies and intensities similar to those of Cu^{II}-LADH and the NADH complex, in particular. Their ~310-cm^{-1} peaks are largely obscured by the ice mode at ~309 cm^{-1}. The ~260-cm^{-1} metal–imidazole mode is clearly present in Ni^{II}-LADH but appears not to be resonance-enhanced in Fe^{III}-LADH. Addition of D_2O or varying the pH between 7 and 10 had no significant effect on the Raman peak positions of Fe^{III}-LADH. For both Ni^{II}-LADH and Fe^{III}-LADH the greatest Raman intensities were achieved at excitation wavelengths closest to their principal absorption maxima. Zn^{II}-LADH yielded only the Raman spectrum of the frozen solvent in this frequency range, similar to the low-temperature H_2O spectrum shown in Figure 8.

The RR spectrum of Fe^{III}-LADH also contains several peaks in the 700–900-cm^{-1} region (data not shown). The strongest feature is a sharp peak at 746 cm^{-1} that is observed close to this frequency in the Cu^{II}-LADH spectra. Since we and others[35] have observed a peak at 746 cm^{-1} in the Raman spectrum of native Zn^{II}-LADH, it is most likely due to a protein mode. The 746-cm^{-1} peak of Fe^{III}-LADH is accompanied by less intense bands at 783 and 812 cm^{-1} that we attribute to combinations of the fundamentals: 357 + 428 = 785 cm^{-1} and 387 + 428 = 815 cm^{-1}.

Cobalt(II)-substituted LADH has an intense absorption maximum at 350 nm[19a] which is attributable to a cysteine S → Co(II) CT transition by analogy to the behavior of other Co(II)-substituted blue copper proteins and model compounds.[28] Excitation of a ~3 mM Co^{II}-LADH solution at 363.8 nm or a ~10 mM crystalline suspension at 350.7 nm failed to yield any resonance-enhanced modes. Similarly, no RR spectra could be obtained from the Co^{II}-LADH/NAD^+/pyrazole complex by using excitation at 406.7, 530.9, and 647.1 nm. We also experienced difficulty with the cobalt(II) model compound, $Co[SC(CH_3)_2CH_2NH_2]_2$,[18] whose tetrahedral coordination to two thiolate sulfurs and two amine nitrogens most closely mimics the coordination of cobalt in the Co^{II}-LADH/NAD^+/pyrazole complex. No resonance-enhanced modes were observed with visible excitation, and only weakly enhanced modes (3- to 5-fold intensity increases) were observed with 363.8-nm excitation. These modest intensity increases occurred at 218, 266, 350, and 383 cm^{-1}, but not at 245 cm^{-1}, in contrast to an earlier report on this compound.[36a] Moreover, the failure to observe any histidine-dependent RR bands in Co^{II}-LADH is disappointing in view of the significant enhancement of Co–N vibrations by excitation within the visible absorption bands of Co(II)–imidazole[36b] and Co(II)–thiocyanate[36c] complexes.

Discussion

Crystallographic studies have indicated that the structure of LADH lacking its catalytic zinc ions is nearly identical with the structure of native LADH.[3b] Similarly, the metal binding site of plastocyanin is preformed in apoplastocyanin.[4] Both of these proteins appear to provide a near-tetrahedral binding site for a variety of metal ions.[3,37] This is substantiated for Fe(III)-, Ni(II)-, and Cu(II)-substituted alcohol dehydrogenases by the appearance of a set of resonance Raman peaks between 350 and 420 cm^{-1} whose strong enhancements appear to be characteristic of tetrahedral coordination. The high energies of these metal–cysteinate vibrational modes are best explained by the presence of an unusually short metal-to-sulfur bond (<2.2 Å) at the metal site. A short zinc-to-sulfur bond has also been indicated in the crystal structure of native Zn-LADH (Figure 1). The lack of inorganic model complexes which mimic the spectroscopic properties of blue copper sites may be due in part to the difficulty of creating Cu(II) species with short Cu–S bonds, as well as tetrahedral geometry. Thus, Cu^{II}-LADH must be considered an extremely useful analogue for the interpretation of a variety of spectroscopic information relating to blue copper proteins.

Binding of either coenzymes or inhibitors to Cu^{II}-LADH has marked effects on its spectroscopic properties, most likely the result of changes in coordination geometry at the metal center. In binary complexes with inhibitors (e.g., pyrazole, imidazole, β-mercaptoethanol, and cyanide), Cu^{II}-LADH shows a decrease in its absorption maximum from 570 to ~500 nm, an increase in the EPR hyperfine splitting from 50 to ~120 ($\times 10^{-4}$ cm^{-1}), and a loss of intensity in the Cu–cysteinate RR peaks between 350 and 420 cm^{-1}. All three of these changes are suggestive of a distortion away from tetrahedral and toward a more planar structure. In contrast, addition of coenzymes (e.g., NAD^+ or NADH) which push the protein into the closed conformation appears to have the opposite effect of shifting the copper site toward a more nearly tetrahedral geometry. Thus, the absorption maximum increases from 570 to ~690 nm, the EPR hyperfine splitting decreases from 50 to ≤30 ($\times 10^{-4}$ cm^{-1}), and the RR peaks between 350 and 420 cm^{-1} increase substantially in intensity. All of these characteristics of the Cu^{II}-LADH coenzyme complexes are typical of blue copper centers.

The close resemblance of Cu(II)-substituted LADH and the blue copper proteins is further demonstrated by their Raman excitation profiles which indicate that a single σS(Cys) → Cu(II) charge-transfer transition is responsible for resonance enhancement. The RR spectra of the various forms of Cu^{II}-LADH exhibit five to eight peaks in the 320–450-cm^{-1} region compared to at least nine resolvable peaks between 330 and 470 cm^{-1} in the blue copper proteins such as azurin and stellacyanin which contain only a single cysteine ligand.[12–14] Since there is no indication of a greater number of cysteine contributions to either the RR spectrum or the enhancement profile of Cu^{II}-LADH compared to the blue copper proteins, either the two cysteine residues in Cu^{II}-LADH have very similar properties or only one of the cysteines is participating. The fact that the molar extinction coefficient for Cu^{II}-LADH of ~4000 M^{-1} cm^{-1} per Cu is close to the typical values of ~3500 M^{-1} cm^{-1} per Cu in azurins and stellacyanins[8,12] argues for only one cysteinate contributing substantially to the 620-nm CT band in the Cu^{II}-LADH system. Electronic spectroscopic studies of Cu^{II}-LADH at low temperature (Figure 3) reveal a higher energy feature in addition to the ~610-nm band which could be due to the S → Cu CT transition of a second cysteinate.[30] This would imply that only one of the cysteinates in Cu^{II}-LADH is responsible for the resonance enhancement of the vibrational spectrum.

In addition to an overabundance of resonance-enhanced Cu–L vibrations, a further characteristic of both Cu^{II}-LADH and the blue copper proteins is the smaller than expected copper isotope dependence for many of these modes. It is likely that most of these resonance-enhanced modes represent mixtures of vibrational components, i.e., coupled stretching and bending motions involving a number of different ligand atoms.[12–15] Candidates for such admixing are ν(Cu–S), δ(S–$C_β$–$C_α$), and δ(Cu–S–$C_β$) of cysteine and ν(Cu–Im) and δ(imidazole) of histidine. Coupling of these modes may well be related to the rigidity imposed on the copper center by the protein (described by such concepts as entatic state[38] or rack-induced bonding[39]). The actual means by which all of these vibrational modes become enhanced through the cysteinate S → Cu(II) charge-transfer transition is uncertain but could be due either to their vibrational mixing with the Cu–S stretch or to the involvement of several ligand molecular orbitals in the excited-state distortion which accompanies the electronic transition.[13] In any case, the present study on the RR spectrum of Cu^{II}-LADH and its binary and ternary complexes has demonstrated that the copper site in this protein is subject to the same kinds of constraints as in the blue copper proteins.

Another feature shared by Cu^{II}-LADH and the blue copper proteins is that many of the Cu–L vibrational modes between 320 and 450 cm^{-1} are affected by deuterium isotope substitution. In

(35) Yue, K. T.; Yang, J.-P.; Martin, C. L.; Sloan, D. L.; Callender, R. H. *Biochem. Biophys. Res. Commun.* **1984**, *122*, 225.
(36) (a) Salama, S.; Schugar, H.; Spiro, T. G. *Inorg. Chem.* **1979**, *18*, 104. (b) Salama, S.; Spiro, T. G. *J. Am. Chem. Soc.* **1978**, *100*, 1105. (c) Chottard, G.; Bolard, J. *Chem. Phys. Lett.* **1975**, *33*, 309.
(37) Hauenstein, B. L., Jr.; McMillin, D. R. *Met. Ions Biol. Syst.* **1981**, *13*, 319.
(38) Williams, R. J. P. *Inorg. Chim. Acta Rev.* **1971**, *5*, 137.
(39) Gray, H. B.; Malmström, B. G. *Comments Inorg. Chem.* **1983**, *2*, 203.

azurins and stellacyanin, six to seven of the nine peaks in this region shift to lower energy upon deuteration.[12b,14] Although few of the peaks in Cu^{II}-LADH or Cu^{II}-LADH/pyrazole show any observable deuterium isotope dependence, in the NADH complex (which is most like a blue copper protein), six of the eight peaks have significantly altered frequencies or intensities in D_2O. The deuterium isotope effects in the blue copper proteins have previously been attributed to the coupling of Cu-L modes with imidazole ring vibrations.[13] However, the large changes in peak intensities and upward shifts in frequency observed for the Cu^{II}-LADH/NADH complex requires a more extensive explanation. For example, these deuterium isotope effects could arise from hydrogen-bonding interactions between the ligating cysteine sulfur atom and hydrogen donor groups of other protein residues. We have observed such anomalous, deuterium-induced intensity and frequency changes in the hydrogen-bonded Fe-O-Fe center of hemerythrin.[40]

Hydrogen bonding of metal-coordinated sulfur atoms is a general phenomenon in sulfur-containing metalloproteins. In the crystal structures of mononuclear, binuclear, and tetranuclear iron-sulfur proteins, almost every sulfur ligand is involved in at least one NH···S or OH···S hydrogen bond to the protein, with the majority arising from peptide NH groups.[41,42] Variations in the extent of hydrogen bonding may explain differences in redox potentials for different iron-sulfur clusters.[41,43] Similarly, in the crystal structures of blue copper sites, each of the cysteine ligands appears to be involved in at least one hydrogen bond between the sulfur atom and the protein backbone. Thus, in plastocyanin there is a hydrogen bond between Cys-84 and the amide NH of residue 38,[5a] in azurin from *A. denitrificans* Cys-112 is hydrogen bonded to the NH of residue 47,[5c] and in azurin from *Pseudomonas aeruginosa* a hydrogen bond is also likely to occur between Cys-112 and the NH of residue 47.[5b,d] Copper-substituted alcohol dehydrogenase may well be an analogous case since the crystal structure of the zinc enzyme indicates that Cys-46 is hydrogen bonded to the amide NH of residue 48.[44] These hydrogen bonds undoubtedly play a role in enforcing the unusual geometry of the blue copper sites and may also explain the unusual deuterium isotope dependences in their resonance Raman spectra.

Acknowledgment. We particularly thank Dr. Eila Cedergren, Dr. Michael Zeppezauer, and Dr. William Woodruff for their helpful discussions and comments. This research was supported by the National Institutes of Health (GM18865), a NATO Travel Grant (921/83), the Deutsche Forschungsgemeinschaft, and the Bundesministerium für Forschung und Technologie.

Registry No. LADH, 9031-72-5; NADH, 58-68-4; NAD, 53-84-9; Cu, 7440-50-8; Ni, 7440-02-0; Co, 7440-48-4; Fe, 7439-89-6; S, 7704-34-9; $HO(CH_2)_2OH$, 60-24-2; CN^-, 57-12-5; pyrazole, 288-13-1; imidazole, 288-32-4.

(40) Shiemke, A. K.; Loehr, T. M.; Sanders-Loehr, J. *J. Am. Chem. Soc.* **1986**, *108*, 2437.
(41) Adman, E.; Watenpaugh, K. D.; Jensen, L. H. *Proc. Natl. Acad. Sci. U.S.A.* **1975**, *72*, 4854.
(42) Tsukihara, T.; Fukuyama, K.; Nakamura, M.; Katsube, Y.; Tanaka, N.; Kakudo, M.; Wada, K.; Hase, T.; Matsubara, H. *J. Biochem.* **1981**, *90*, 1763.
(43) Krishnamoorthi, R.; Markely, J. L.; Cusanovich, M. A.; Przysiecki, C. T.; Meyer, T. E. *Biochemistry* **1986**, *25*, 60.
(44) Eklund, H., personal communication.

An Approach toward the Complete FAB Analysis of Enzymic Digests of Peptides and Proteins

Stephen Naylor, A. Frederick Findeis, Bradford W. Gibson, and Dudley H. Williams*

Contribution from the University Chemical Laboratory, Cambridge, CB2 1EW, UK.
Received February 18, 1986

Abstract: A current limitation in the use of FAB mass spectrometry for mixture analysis is that some components of the mixture, dissolved in matrices such as glycerol, are not normally observed. Three enzymic digestions (one of a polypeptide and two of small proteins) are used to show that it is the hydrophilic peptides in a mixture that are suppressed. By determination of the FAB spectra of both pure hydrophilic and hydrophobic peptides, and of mixtures of these, it is shown that (i) hydrophilic peptides alone give a relatively poor signal response and (ii) hydrophilic peptides are further suppressed in the presence of hydrophobic peptides that initially occupy the surface of the matrix. A hydrophilicity/hydrophobicity index (ΔF values) can be used to indicate which peptide may be suppressed. Suppression may be reduced by HPLC partial fractionation or the conversion of polar carboxyl groups to more hydrophobic ester derivatives.

The determination of the molecular weights of relatively large polar molecules has been facilitated enormously since the discovery of fast atom bombardment (FAB) mass spectrometry.[1] Additionally, since the advent of genetic engineering and rapid DNA-sequencing techniques, there is an increased demand for efficient methods to check the accuracy of an assumed protein sequence. This demand arises because mistakes can be made in reading DNA-sequencing gels or because posttranslational modifications of proteins that are normally present may be absent when the product is engineered in a bacterial cell. It has been demonstrated that such rapid checking of protein sequences can be achieved by digesting the protein enzymically and determining by FAB mass spectrometry the molecular weights of the peptides in the resulting mixture.[2-7] However, a limitation of this powerful method has been that, in a complex mixture, not all the peptide fragments are seen. In view of the importance of the technique,

(1) Barber, M.; Bordoli, R. S.; Sedgwick, R. D.; Tyler, A. N. *J. Chem. Soc., Chem. Commun.* **1981**, 325.
(2) Morris, H. R.; Panico, M.; Taylor, G. W. *Biochem. Biophys. Res. Commun.* **1983**, *117*, 299.
(3) Wada, Y.; Hayashi, A.; Fujita, T.; Matsuo, T.; Kaiakuse, I.; Matsuda, H. *Int. J. Mass Spectrom. Ion Phys.* **1983**, *48*, 209.
(4) Takao, T.; Yoshida, M.; Hong, Y.-M.; Aimoto, S.; Shimonishi, Y. *Biomed. Mass Spectrom.* **1984**, *11*, 299.
(5) Gibson, B. W.; Biemann, K. *Proc. Natl. Acad. Sci. U.S.A.* **1984**, *81*, 1956.
(6) Wada, Y.; Hayashi, A.; Katakuse, I.; Matsuo, T.; Matsuda, H. *Biomed. Mass Spectrom.* **1985**, *12*, 122.
(7) Clench, M. R.; Garner, G. V.; Gordon, D. B.; Barber, M. *Biomed. Mass Spectrom.* **1985**, *12*, 355.

0002-7863/86/1508-6359$01.50/0